

Compromise between conjugation length and charge-transfer in nonlinear optical η^5 -monocyclopentadienyliron(II) complexes with substituted oligo-thiophene nitrile ligands: Synthesis, electrochemical studies and first hyperpolarizabilities

M. Helena Garcia ^{a,b,*}, Paulo J. Mendes ^{b,c}, M. Paula Robalo ^{b,d}, A. Romão Dias ^b, Jochen Campo ^e, Wim Wenseleers ^{e,*}, Etienne Goovaerts ^e

^a Faculdade de Ciências da Universidade de Lisboa, Ed.C8, Campo Grande, 1749-016 Lisboa, Portugal

^b Centro de Química Estrutural, Instituto Superior Técnico, Universidade Técnica de Lisboa, Av. Rovisco Pais, 1049-001 Lisboa, Portugal

^c Centro de Química de Évora, Universidade de Évora, Rua Romão Ramalho 59, 7002-554 Évora, Portugal

^d Departamento de Engenharia Química, Instituto Superior de Engenharia de Lisboa, Rua Conselheiro Emídio Navarro, 1, 1959-007 Lisboa, Portugal

^e Department of Physics, University of Antwerp, Campus Drie Eiken, Universiteitsplein 1, B-2610 Wilrijk-Antwerpen, Belgium

Received 12 February 2007; received in revised form 17 March 2007; accepted 17 March 2007

Available online 23 March 2007

Abstract

A systematic series of η^5 -monocyclopentadienyliron(II) complexes with substituted oligo-thiophene nitrile ligands of general formula $[\text{FeCp}(\text{P}_\text{P})(\text{NC}\{\text{SC}_4\text{H}_2\}_n\text{NO}_2)] [\text{PF}_6]$ (P_P = dppe, (+)-diop; n = 1–3) has been synthesized and characterized. The electrochemical behaviour of the new compounds was explored by cyclic voltammetry. Quadratic hyperpolarizabilities (β) of the complexes with dppe coligands have been determined by hyper-Rayleigh scattering (HRS) measurements at two fundamental wavelengths of 1.064 and 1.550 μm , to uncover the two-photon resonance effect and to estimate static β values. The obtained overall results are found to be better than for the related η^5 -monocyclopentadienyliron(II) complexes with *p*-benzonitrile derivatives. Although an increase of the resonant β at 1.064 μm with increasing number of thiophene units in the conjugated ligand was found (up to 910×10^{-30} esu), the static values β_0 remain practically unchanged, as shown by the 1.550 μm measurements. Combined with the electrochemical and spectroscopic data (IR, NMR, UV–vis), this remarkable evolution of β shows that the increase of conjugation length is balanced by a decrease in charge-transfer efficiency.

© 2007 Published by Elsevier B.V.

Keywords: Iron complexes; Thiophene nitrile ligands; Cyclic voltammetry; Nonlinear optics; Quadratic hyperpolarizabilities; Molecular first hyperpolarizabilities

1. Introduction

Organometallic compounds have given rise to a great deal of interest owing to their application in the field of

nonlinear optics (NLO) [1–6]. For second-order nonlinear optics, strongly asymmetric systems are needed, which led to the development of typical push–pull systems in which the metal centre, bound to a highly polarizable conjugated backbone, acts as an electron releasing or withdrawing group. The strong charge-transfer (CT) transitions occurring in organometallic compounds are expected to lead to high molecular first hyperpolarizabilities β . In addition, the position of the CT band, usually at visible wavelengths, can be tuned by variation of the ligands and/or the metal

* Corresponding authors. Address: Faculdade de Ciências da Universidade de Lisboa, Ed.C8, Campo Grande, 1749-016 Lisboa, Portugal (M.H. Garcia).

E-mail addresses: lena.garcia@fc.ul.pt (M.H. Garcia), wim.wenseleers@ua.ac.be (W. Wenseleers).

itself, to optimise the hyperpolarizability through (near) resonant enhancement. After the initial interesting results achieved with ferrocene systems [7,8], a further improvement of the NLO response was obtained with half-sandwich complexes in which the metal centre is coplanar with the π -conjugated backbone. Concerning this feature, systematic studies were made on η^5 -monocyclopentadienylmetal complexes presenting benzene-based conjugated ligands bound to the metal centre through nitrile or acetylide linkages [9–13]. Ruthenium and iron organometallic moieties were found to be much more efficient donor groups for second-order NLO purposes than the traditional organic donor groups (NMe₂, NH₂, etc.), leading to higher β values.

It is well known that the quadratic hyperpolarizability of purely organic push–pull molecules increases strongly with the length of the conjugated chain [14,15]. A previous attempt to exploit this effect in nitrile metal complexes, by replacing a phenyl by a biphenyl unit, was unsuccessful due to the significant torsion angle in the latter ligand, breaking the conjugation [9]. The much higher β value obtained when the conjugation length is increased without affecting planarity by insertion of a vinylene unit, further supported this assumption. The effect of the phenylene-phenylene dihedral angle on β has been examined theoretically for comparable Ru complexes [16]. For oligo-thiophene derived ligands, however, an improved planarity can be expected from the limited sterical hindrance as compared to oligo-phenyls. Although an ab initio calculation by Ciofalo and La Manna [17] suggest that even for terthiophene the gas-phase structure is not planar, they found a very low energy barrier for conformational inter-conversion and as a result the geometry is very sensitive to the chemical environment. This is further illustrated by a semi-empirical calculation by Porter et al. [18], which indicates that the structure of bithiophene becomes planar in aqueous solution. Therefore, it seems fair to assume a negligible effect of non-planarity in the present thiophene-based complexes, especially because the oligo-thiophene is incorporated in a push–pull system which should favour a more planar structure. Thiophene chains are also known to provide a higher level of electronic coupling than benzenoid-based structures because of their more effective conjugation thus yielding a good basis for high second-order NLO responses. Therefore, we now study the conjugation-length dependence of the first hyperpolarizability in a series of iron cyclopentadienyl compounds incorporating thiophene derived ligands. Although some reports concerning the NLO properties of thiophene-based organometallic complexes have been published, they are mainly about ferrocenyl and tricarbonyl chromium arene derivatives [19–25] in which the metal is unfavourably placed outside of the conjugation plane [7], in contrast to the present complexes.

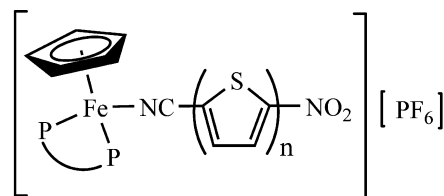
In this work, we report the synthesis, characterization and electrochemical studies of a systematic series of η^5 -monocyclopentadienyliron complexes with nitro-substituted thiophene nitrile ligands of general formula

[FeCp(P₂P)(NC{SC₄H₂})_nNO₂][PF₆] (P₂P = dppe, (+)-diop; $n = 1$ –3). The chiral (+)-diop coligand is used to favour the formation of a non-centrosymmetrical crystal structure, required for macroscopic second-order NLO. Quadratic hyperpolarizabilities (β) for the complexes with dppe have been determined by hyper-Rayleigh scattering (HRS) measurements at two different wavelengths of 1.064 and 1.550 μm , to reveal the effect of (near) resonant enhancement. The least resonant β values (i.e. at 1.550 μm) can be used to obtain more dependable static values β_0 , enabling the formulation of structure–NLO property relationships. Spectroscopic data are used in order to evaluate the effect of the type of phosphine coligand and the length of the conjugated ligand on the second-order NLO response of the complexes, which is compared to the observations for the *p*-benzonitrile analogues. Cyclic voltammetry is also used as a tool for a better understanding of the electronic factors responsible for the NLO behaviour of the compounds studied in this work.

2. Results and discussion

The thiophene chromophores were synthesized according to general procedures. 5-Nitrothiophene-2-carbonitrile (**L1**) was prepared as described in the literature [26]. 5'-Nitro-2,2'-bithiophene-5-carbonitrile (**L2**) and 5''-nitro-2,2':5',2''-terthiophene-5-carbonitrile (**L3**) were prepared by nitration of the previously synthesized 2,2'-bithiophene-5-carbonitrile and 2,2':5',2''-terthiophene-5-carbonitrile, respectively, with a clay-supported cupric nitrate (*claycop*) in Menke conditions (see Section 4).

The complexes (Fig. 1) were prepared by iodide abstraction of [FeCp(P₂P)I] (P₂P = dppe or (+)-diop, dppe = 1,2-bis(diphenylphosphino)ethane, diop = 2,3-*O*-isopropylidene-2,3-dihydroxy-1,4-bis(diphenylphosphino)butane) with TIPF₆ in the presence of an excess of the appropriate thiophene derivative in dichloromethane at room temperature. After workup, reddish microcrystalline products of [FeCp(P₂P)(NC{SC₄H₂})_nNO₂][PF₆] (P₂P = dppe, $n = 1$ (**1a**), $n = 2$ (**2a**), $n = 3$ (**3a**); P₂P = (+)-diop, $n = 1$ (**1b**), $n = 2$ (**2b**), $n = 3$ (**3b**)) were obtained with yields in the range of 28–56%. The compounds are quite stable towards oxidation in air and to moisture both in the solid state and in solution. Formulation of the new compounds was supported by analytical data, IR and ¹H, ¹³C and ³¹P NMR spectra. The molar conductivities of ca. 10^{−3} M solutions



P₂P = dppe: $n = 1$ (**1a**), $n = 2$ (**2a**), $n = 3$ (**3a**)
 P₂P = (+)-diop: $n = 1$ (**1b**), $n = 2$ (**2b**), $n = 3$ (**3b**)

Fig. 1. Structural formulas of the complexes studied in this work.

of the complexes in nitromethane, in the range of $69\text{--}78 \text{ } \Omega^{-1} \text{ cm}^2 \text{ mol}^{-1}$, are consistent with values reported for 1:1 type electrolytes [27].

Typical IR bands confirm the presence of the cyclopentadienyl coligand (ca. $3100\text{--}3040 \text{ cm}^{-1}$), the PF_6^- anion (840 and 550 cm^{-1}) and the coordinated nitrile ($2180\text{--}2210 \text{ cm}^{-1}$) in all the complexes. No significant change was observed on $\nu(\text{NC})$ upon coordination of **L3** but in the case of **L1** and **L2**, depending on the coordinated phosphine coligand, negative shifts were found in the range of $5\text{--}45 \text{ cm}^{-1}$. These negative shifts, which indicate enhanced π -backdonation from the metal d orbitals to the π^* orbital of the NC group, are higher than those found in the related *p*-benzonitrile derivatives [10,28]. As the number of thiophene rings in the ligands increases, the shift of $\nu(\text{NC})$ upon coordination was found to become less negative. So apparently, the CT through the long conjugated ligand is hampered, which has an unfavourable effect on the molecular first hyperpolarizability β (see below).

^1H and ^{13}C NMR resonances for the cyclopentadienyl ring are in the range usually observed for monocationic iron(II) complexes and seem to be affected by the phosphine coligand but are relatively insensitive to the nature of the aromatic nitrile. For the nitrile ligands, the effect on NMR resonances upon coordination is mainly found in the deshielding observed at the carbon of the NC functional group, which magnitude depends on the phosphine coligand and the nature of the coordinated nitrile. The observed deshielding is lower for the complexes with dppe than for the ones with (+)-diop coligand and for the nitrile ligands with less extended aromatic system. This behaviour agrees with the proposed π -backdonation interaction inferred from the IR spectra which indicates a decreased π -backdonation with increasing the number of thiophene rings in the ligands. The deshielding observed for the complexes containing **L1** and **L2** derivatives are lower than those found in the related *p*-benzonitrile complexes [10,28], which can be a result of the enhanced π -backdonation in the present compounds with thiophene ligands.

^{31}P NMR data of the complexes showed the expected deshielding of the phosphines upon coordination. The dppe ligand was characterized by a singlet and (+)-diop by two doublets due to its inequivalent phosphorus atoms. The deshielding effect upon coordination was enhanced with the better donor character of the phosphine, showing an easier release of electron density towards the metal centre. No significant changes on the phosphorus electron density were observed by the presence of different coordinated thiophenes.

The optical absorption spectra of all complexes were recorded using $5.0 \times 10^{-5} \text{ M}$ solutions in dichloromethane. The spectra for the dppe complexes **1a–3a** typify the behaviour of the compounds studied in this work (Fig. 2) and the optical data are summarized in Table 1. The spectra of all compounds are characterized by the presence of intense absorption bands which can be assigned based on the spectra of the free ligands and the organometallic fragment

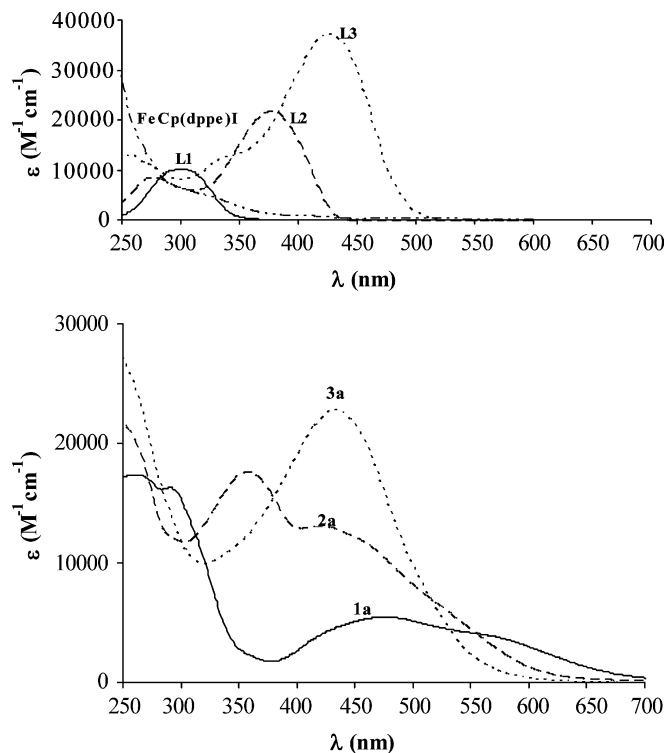
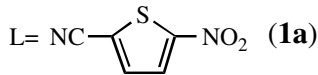
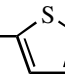
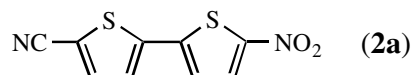
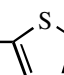
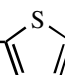

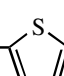
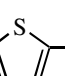
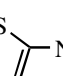
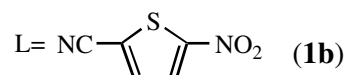
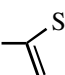
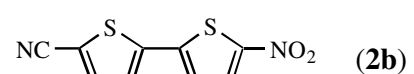
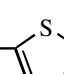
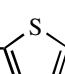
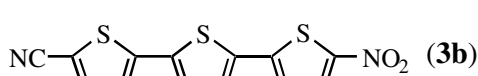
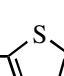
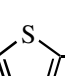
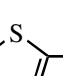


Fig. 2. Absorption spectra of $[\text{FeCp}(\text{dppe})(\text{NC}\{\text{SC}_4\text{H}_2\}_n\text{NO}_2)][\text{PF}_6]$ ($n=1$: **1a**, $n=2$: **2a**, $n=3$: **3a**) recorded in CH_2Cl_2 ($5.0 \times 10^{-5} \text{ M}$). (Top) Absorption spectra for the free thiophene ligands $\text{NC}\{\text{SC}_4\text{H}_2\}_n\text{NO}_2$ ($n=1$: **L1**, $n=2$: **L2**, $n=3$: **L3**) and $\text{FeCp}(\text{dppe})\text{I}$ in the same experimental conditions.

$[\text{FeCp}(\text{P}_2)]^+$. For all the complexes **1a–3a** the electronic transition of the metallic moiety ($\lambda \sim 260 \text{ nm}$) and the uncoordinated thiophene ligands ($\lambda \sim 290\text{--}440 \text{ nm}$) can be clearly recognized. Furthermore, compounds **1a** and **2a** with one and two thiophene rings exhibit a separate metal-to-ligand charge transfer (MLCT) band(s) in the visible region ($\lambda \sim 400\text{--}650 \text{ nm}$). This is, however, not the case for the compound with three thiophenes **3a**, where the MLCT band is very probably overlapped with the intense absorption band attributed to the $\pi\text{--}\pi^*$ transition occurring in the coordinated thiophene ligand **L3**. The energies of the MLCT bands are lower than those found in the related *p*-benzonitrile complexes, which can lead to an increase of the resonance enhancement of β , but also of the static values β_0 . Clearly, the chain-lengthening leads to a bathochromic shift of the transitions of the conjugated ligand and a hypsochromic shift of the MLCT band. The latter effect was also observed for the related *p*-benzonitrile compounds [10,28] and was explained on the basis of a breaking of the conjugation due to the presence of a significant torsion angle between the aromatic rings. For the present thiophene derivatives, however, the conjugated chain is expected to be more planar because of the limited sterical hindrance between the successive thiophene rings. So here the hypsochromic shift indicates a lowering of the CT efficiency with increasing length of the conjugated chain, which has a detrimental effect on β .

Table 1
Optical data for complexes [FeCp(P_P)(NC{SC₄H₂}_nNO₂)] [PF₆] in dichloromethane solution (ca. 5.0 × 10⁻⁵ mol dm⁻³)

Compound [FeCp(P _P)L] [PF ₆]	λ (nm)	ε × 10 ⁴ (M ⁻¹ cm ⁻¹)
<i>P</i> _P = <i>dpp</i> e		
 L = NC—  —NO ₂ (1a)	263 (sh)	
	290	1.71
	475	0.59
	570 (sh)	
 NC—  —  —NO ₂ (2a)	256 (sh)	
	358	1.70
	423	1.24
	530 (sh)	
 NC—  —  —  —NO ₂ (3a)	254 (sh)	
	437	2.40
<i>P</i> _P = (+)- <i>diop</i>		
 L = NC—  —NO ₂ (1b)	272 (sh)	
	292	2.48
	500	0.75
 NC—  —  —NO ₂ (2b)	258 (sh)	
	360	1.49
	450	0.97
 NC—  —  —  —NO ₂ (3b)	255 (sh)	
	431	2.16

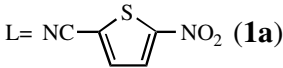
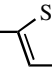
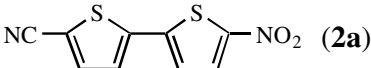
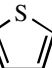
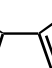
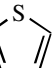
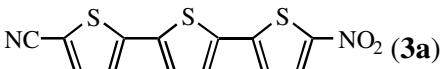
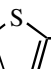
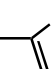
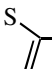
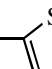
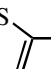
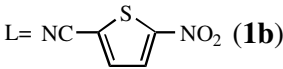
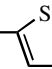
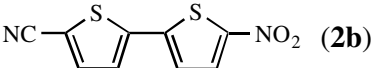
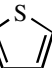
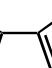
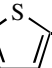
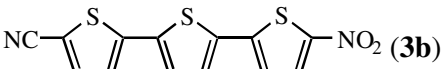
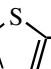
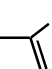
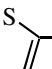
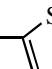
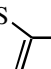
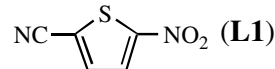
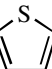
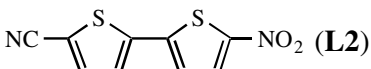
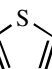
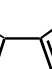
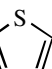
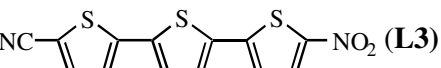
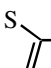
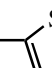
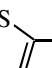
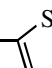
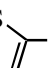
In order to study the solvatochromic behaviour of all the compounds, absorption spectra were measured in different solvents of increasing polarity (chloroform, methanol, acetone, nitromethane and dimethylformamide). Although the data must be carefully analyzed due to the broad and composite structure of the bands, which lead to some uncertainty in the attribution of λ_{max} values, the studies show a slight bathochromic shift on the MLCT bands upon increasing solvent polarity. This positive solvatochromic behaviour exhibited by these compounds is characteristic of electronic transitions with an increase of the dipole moment upon (photo-)excitation. The positive shift seems to increase from compound **1** to compound **2** but much less solvatochromic effect could be detected for the complexes with three thiophene rings (**3**). In all studied solvents, with dipolar moments in the range 1.1–3.8 D, a single structureless band was found for complexes **3a** and **3b** without evidence of any shoulder. The reason for this might be the overlapping of the MLCT and the ligand π – π^* bands. In fact, the MLCT band seems to shift to higher energies and the intra-ligand band to lower energies with increasing conjugation length and both are overlapped completely for the compounds with three thiophene rings.

In order to obtain an insight on the electron richness of the organometallic fragment, the electrochemical behaviour of all the compounds was studied by cyclic voltammetry in dichloromethane and acetonitrile between the limits imposed by the solvents. As an example, the cyclic voltammetry response of **2a** in dichloromethane is shown in Fig. 3, and the most relevant data for the redox changes exhibited by all the complexes in dichloromethane are summarized in Table 2.

The electrochemical behaviour of the compounds in dichloromethane is characterized by the presence of one quasi-reversible redox wave attributed to Fe(II)/Fe(III) oxidation, in the range 0.78–1.06 V, and two quasi-reversible or irreversible waves attributed to reduction processes occurring on the coordinated nitrile ligands, in the range –0.58 to –0.91 V for redox process A and –1.19 to –1.27 V for redox process B. Additionally, redox waves with low intensity were found and attributed to the decomposition products after both reductive processes. A first anodic shoulder C was found at $E_{\text{pa}} \approx -0.8$ V and originated from the first reduction on the coordinated ligand. A second wave D at $E_{\text{p}/2} \approx -1.3$ V and a third cathodic wave E at $E_{\text{pc}} \approx -0.9$ V appeared after the second reduc-

Table 2

Electrochemical data for the complexes $[\text{FeCp}(\text{P}_\text{P})(\text{NC}\{\text{SC}_4\text{H}_2\}_n\text{NO}_2)][\text{PF}_6]$ and the corresponding thiophene ligands $\text{NC}\{\text{SC}_4\text{H}_2\}_n\text{NO}_2$ in CH_2Cl_2 solution at 20 °C

Compound $[\text{FeCp}(\text{P}_\text{P})\text{L}][\text{PF}_6]$	E_{pc} (V)	E_{pa} (V)	$E_{\text{p}/2}$ (V)	$E_{\text{pa}} - E_{\text{pc}}$ (mV)	$I_{\text{c}}/I_{\text{a}}$
P_P = dppe					
 L = NC-  -NO ₂ (1a)	0.84	0.91	0.88	70	1.0
	-0.66	-0.58	-0.62	80	0.9
	-1.29	-1.05	-	-	-
 NC-  -  -  -NO ₂ (2a)	0.77	0.85	0.81	80	1.0
	-0.86	-0.78	-0.82	80	1.0
	-1.28	-1.20	-1.24	80	0.8
 NC-  -  -  -  -  -NO ₂ (3a)	0.74	0.81	0.78	70	1.0
	-0.94	-0.87	-0.91	70	0.9
	-1.31	-1.23	-1.27	80	0.6
P_P = (+)-diop					
 L = NC-  -NO ₂ (1b)	1.02	1.09	1.06	70	0.9
	-0.61	-0.54	-0.58	70	0.9
	-1.24	-1.02	-	-	-
 NC-  -  -  -NO ₂ (2b)	0.94	1.01	0.98	70	0.9
	-0.82	-0.74	-0.78	80	0.9
	-1.23	-1.14	-1.19	90	0.9
 NC-  -  -  -  -  -NO ₂ (3b)	0.90	0.98	0.94	80	0.9
	-0.94	-0.86	-0.90	80	0.6
	-1.23	-1.15	-1.19	80	0.8
Ligand					
 NC-  -NO ₂ (L1)	-0.74	-0.66	-0.70	80	1.0
	-1.59	-1.23	-	-	-
 NC-  -  -  -NO ₂ (L2)	-0.88	-0.80	-0.84	80	0.9
	-1.42	-1.27	-	-	-
 NC-  -  -  -  -  -NO ₂ (L3)	-0.93	-0.86	-0.90	70	0.9
	-1.43	-1.30	-	-	-

tive process. Moreover, a low anodic wave **F** at -0.15 V arises only if the potential reaches the second reductive process. This behaviour is illustrated by Fig. 3, which shows that the waves **E** and **F** are not present if the potential is reversed immediately after the first reductive process.

The Fe(II)/Fe(III) potential is affected both by the phosphine coligand and the nature of the coordinated nitrile ligand. Replacing the dppe coligand by (+)-diop results in an increase of the redox potential of the Fe(II)/Fe(III) couple, which agrees with the relative donating ability of

the two phosphines to the metal centre. For the same phosphine, the Fe(II)/Fe(III) couple potential decreases with the chain-lengthening of the thiophene ligand, which can be due to a less effective release of electronic density from the metal centre to the nitro-acceptor group with the extension of the aromatic system. This indicates that adding more thiophene units in the π -conjugated chain will not necessarily lead to an increase of the molecular β value, which is indeed confirmed by the NLO experiments (see below). These results confirm the evidences of the

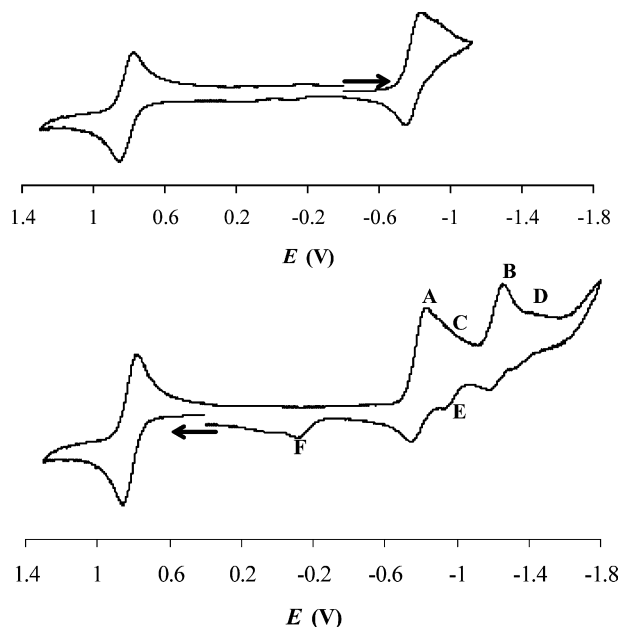


Fig. 3. Cyclic voltammograms of **2a** in CH_2Cl_2 containing 0.1 M $n\text{-Bu}_4\text{NPF}_6$ (sweep rate = 200 mV/s). (Top) Oxidative and the first reductive processes.

spectroscopic data discussed above, namely the relative magnitude of the metal–ligand backdonation, which was found to be smallest for the compounds with three thiophene rings. The Fe(II)/Fe(III) redox couple potentials of this family of compounds are higher than those observed for the related *p*-benzonitrile compounds [10,28] which is in good agreement with the lower electronic density at the metal centre in thiophene derivatives.

As mentioned above, the two main redox processes at negative potentials are attributed to reductions occurring at the coordinated thiophene ligands. The electrochemical data for the free thiophene ligands in dichloromethane are summarized in Table 2. The first wave is reversible or quasi-reversible and corresponds to the formation of the anion radical. Owing to the reversibility of the first wave, the second reduction process can be attributed to a further reduction of the anion radical to the corresponding dianion. The irreversibility of this second redox process indicates a poor stability of the dianion. Upon coordination, the reversibility of the first reduction wave remains almost unchanged when the potential is reversed at -1.1 V. Also, it was found that the second reduction process at the thiophene ligands becomes less irreversible upon coordination. This means that the iron organometallic fragment stabilizes the dianionic thiophene ligand species. The electrochemical data show also that the coordination of the thiophene ligands lowers the corresponding reduction potentials according to the overall electron-withdrawing effect of the organometallic fragment. This effect is more pronounced on the second reduction potentials and also depends on the coordinated phosphine and the chain length of the thiophene ligand. The higher reduction potentials found for complexes with dppe are consistent with the relative donat-

ing ability of the two studied phosphines and agree with the spectroscopic data discussed above. The difference between the two reduction potentials strongly depends on the length of the conjugated ligand. This difference is a measure of the interaction between the two negative charges. For the free thiophene ligands, this difference becomes smaller as the chain length increases. As was already recognized for oligothiophenes reported in the literature, this trend can be explained by a stronger coulombic interaction between negative charges developed by shorter conjugated chains [29]. Upon coordination, this trend remains unchanged but the difference between the two reduction potentials becomes smaller. This observation suggests that the organometallic fragment diminishes the coulombic interaction between the two negative charges, as expected considering the cationic character of the moieties.

The electrochemical studies in acetonitrile, at room temperature, showed a significant difference concerning the oxidative electrochemistry of the studied compounds. In fact, the Fe(II)/Fe(III) redox couple of the complexes with dppe (**1a–3a**) have no cathodic counterpart and a second cathodic wave arises at 0.62 V which value is independent of the coordinated thiophene. However, at -20°C , the cathodic wave of the Fe(II)/Fe(III) redox couple arises and the intensity of the cathodic wave at 0.62 V diminishes. In addition, a small anodic wave at ≈ 0.70 V emerges. As an example, the oxidative electrochemistry response of **1a** in acetonitrile is shown in Fig. 4, and the most relevant data for the redox changes exhibited by all the complexes in this solvent are summarized in Table 3. These results suggest that the 17-electron species $[\text{FeCp}(\text{dppe})(\text{NC}\{\text{SC}_4\text{H}_2\}_n\text{NO}_2)]^{2+}$, formed at the electrode surface at oxidation potential, undergo fast decomposition at room temperature (in an ECC process). The presence of a cathodic wave which value is independent of the coordinated thiophenes suggests that it originates from the decomposition of $[\text{FeCp}(\text{dppe})(\text{NC}\{\text{SC}_4\text{H}_2\}_n\text{NO}_2)]^{2+}$ due to the decoordination of the thiophene ligand and its substitution by acetonitrile solvent molecules, leading to the $[\text{FeCp}(\text{dppe})(\text{NCCH}_3)]^{2+}$ species before the reductive counterpart process. These species are stable enough to undergo a reduction process with $E_{\text{pc}} = 0.62$ V leading to a 18-electron $[\text{FeCp}(\text{dppe})(\text{NCCH}_3)]^+$ complex. In order to confirm this

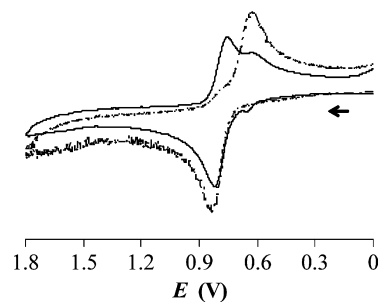
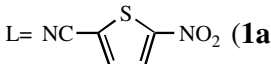
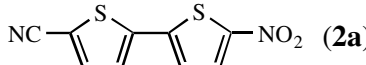
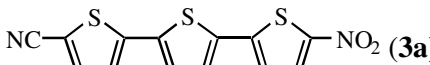
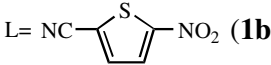
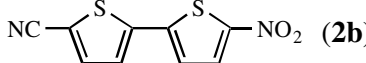
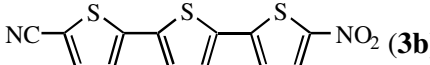
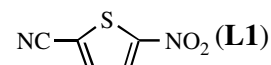
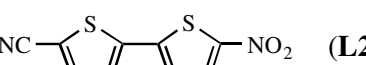
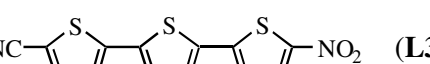


Fig. 4. Cyclic voltammogram of **1a** in NCCH_3 containing 0.1 M $n\text{-Bu}_4\text{NPF}_6$ (sweep rate = 200 mV/s). (-----) 20°C ; (—) -20°C .

Table 3

Electrochemical data for complexes $[\text{FeCp}(\text{P_P})(\text{NC}\{\text{SC}_4\text{H}_2\}_n\text{NO}_2)]^+[\text{PF}_6]^-$ and for the thiophene ligands $\text{NC}\{\text{SC}_4\text{H}_2\}_n\text{NO}_2$ in NCCH_3 solution at -20°C

Compound $[\text{FeCp}(\text{P_P})\text{L}][\text{PF}_6]^a$	E_{pc} (V)	E_{pa} (V)	$E_{\text{p}/2}$ (V)	$E_{\text{pa}} - E_{\text{pc}}$ (mV)	$I_{\text{c}}/I_{\text{a}}$
<i>P_P = dppe</i>					
L =  (1a)	0.76	0.83	0.80	70	0.8
	-0.64	-0.56	-0.60	80	0.9
	-1.22	-1.10	-1.16	120	1.0
 (2a)	0.70	0.76	0.73	60	0.8
	-0.77	-0.71	-0.74	60	1.0
	-1.18	-1.12	-1.15	60	1.0
 (3a)	0.67	0.75	0.71	80	0.8
	-0.84	-0.78	-0.81	60	1.0
	-1.22	-1.16	-1.19	60	1.0
<i>NCCH₃ (4a)</i>					
<i>P_P = (+)-diop</i>					
L =  (1b)	0.93	1.01	0.97	80	0.9
	-0.61	-0.54	-0.58	70	0.9
	-1.31	-1.01	-	-	-
 (2b)	0.84	0.92	0.88	80	0.9
	-0.80	-0.72	-0.76	80	0.9
	-1.16	-1.07	-1.12	90	0.9
 (3b)	0.82	0.90	0.86	80	0.8
	-0.87	-0.79	-0.83	80	0.9
	-1.25	-1.17	-1.21	80	0.9
<i>NCCH₃ (4b)</i>					
<i>Ligand</i>					
 (L1)	-0.70	-0.61	-0.66	90	1.0
	-1.77	-1.40	-	-	-
 (L2)	-0.82	-0.74	-0.78	80	1.0
	-1.38	-1.26	-	-	-
 (L3)	-0.88	-0.81	-0.84	70	1.0
	-1.36	-1.27	-1.32	90	1.0

^a For all the $[\text{FeCp}(\text{P_P})(\text{NC}\{\text{SC}_4\text{H}_2\}_n\text{NO}_2)]^+$ complexes an additional cathodic wave corresponding to reduction of $[\text{FeCp}(\text{P_P})(\text{NCCH}_3)]^{2+}$ species was observed (see text for details).

hypothesis, the complex $[\text{FeCp}(\text{dppe})(\text{NCCH}_3)]^+[\text{PF}_6]^-$ was synthesized and its electrochemistry studied in acetonitrile. The results obtained for the Fe(II)/Fe(III) redox couple are consistent with the formulated hypothesis (see Table 3). The lability of thiophene ligands was also confirmed by ^1H NMR spectroscopic studies. After the electrochemical experiments of the complex **1a**, both the solvent and the supporting electrolyte were removed and the ^1H NMR

spectrum of the sample showed the presence of resonances attributed to both the $[\text{FeCp}(\text{dppe})(\text{NCCH}_3)]^+$ complex and the corresponding free thiophene ligand. The substitution of the thiophene ligands by the acetonitrile solvent in electrochemical experiments during the oxidative process was also observed for the (+)-diop complexes (**1b–3b**) but in a smaller extent. In fact, a small cathodic wave at ≈ 0.79 V was found, which is consistent with the data found

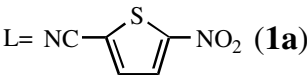
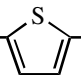
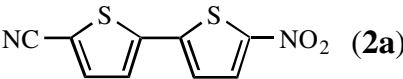
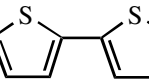
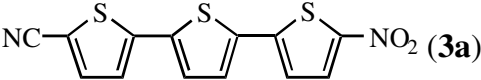
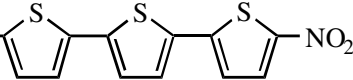
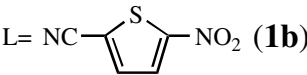
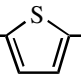
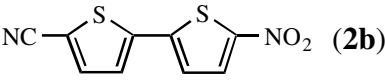
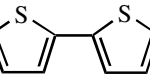
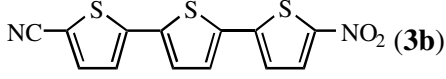
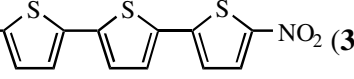
for the complex $[\text{FeCp}(+)\text{-diop}(\text{NCCH}_3)][\text{PF}_6]$ in a separate experiment. This behaviour might be explained by a less favourable kinetic of substitution due to steric crowding around the metal centre as a result of the presence of a bulkier phosphine. The same general trends on oxidation and reduction potentials by varying the phosphine coligand and the nature of nitrile ligands were obtained in acetonitrile. The electrochemical data for the free thiophene ligands in acetonitrile are summarized in Table 3.

In view of the application in second-order nonlinear optics of the compounds studied in this work, it is of interest to consider the HOMO–LUMO gap, as expressed by the difference between the first oxidation and reduction potentials. Extended Hückel MO calculations (EHMO) carried out on similar complexes containing *p*-benzonitrile derivatives show that the HOMO of the complexes is essentially localized in the metal fragment while the LUMO is essentially a pure nitrile ligand orbital [10]. It is reasonable to assume that the character of the HOMO and LUMO remains unchanged for the complexes studied in this work. Hence, the Fe(II)/Fe(III) potential can be related to the rel-

ative magnitude of the HOMO energy. The results discussed above show that the HOMO, as expected, is destabilized by the better electron donor phosphine *dppe* and, to a lower extent, by the chain lengthening of the thiophene ligand. On the other hand, the LUMO, the energy of which can be related to the first reduction potential, is destabilized as the chain-length of the thiophene ligand increases and is only slightly affected by the nature of the phosphine coligand. The difference between the Fe(II)/Fe(III) couple and the first reduction occurring on the thiophene ligand, calculated as an estimation of HOMO–LUMO gap, is shown in Table 4.

The data show that the HOMO–LUMO gaps depend on phosphine coligand, chain lengthening of the thiophene ligand and the solvent used in the electrochemical experiments. As expected, the lower HOMO–LUMO gaps observed for *dppe* complexes are mainly due to the higher energies of the HOMOs since the LUMOs, which are mainly located on thiophene ligands, are only slightly affected by the nature of the phosphine coligand. In fact, as discussed above, replacing the (+)-*diop* coligand by

Table 4
Estimation of HOMO–LUMO gap based on electrochemical data for the complexes $[\text{FeCp}(\text{P}_P)(\text{NC}\{\text{SC}_4\text{H}_2\}_n\text{NO}_2)][\text{PF}_6]$

Compound $[\text{FeCp}(\text{P}_P)\text{L}][\text{PF}_6]$	$E_{\text{ox}} - E_{\text{red}}^{\text{a}}$ (V)	
	CH_2Cl_2	NCCH_3
<i>P</i> _P = <i>dppe</i>		
 L = NC–  –NO ₂ (1a)	1.50	1.40
 NC–  –NO ₂ (2a)	1.63	1.47
 NC–  –NO ₂ (3a)	1.69	1.52
<i>P</i> _P = (+)- <i>diop</i>		
 L = NC–  –NO ₂ (1b)	1.64	1.55
 NC–  –NO ₂ (2b)	1.76	1.64
 NC–  –NO ₂ (3b)	1.84	1.69

^a $E_{\text{ox}} - E_{\text{red}}$ is the difference between the potential of the Fe(II)/Fe(III) redox couple and the first reduction potential occurring on the thiophene ligand.

the better donor dppe phosphine results in a decrease of the redox potential of the Fe(II)/Fe(III) couple, and hence in an increase of the HOMO energies. The chain lengthening of the nitrile ligand leads to an increase in the HOMO–LUMO gap, mainly as a result of the destabilizing effect on the LUMO, as previously discussed. These results are consistent with the electronic spectra discussed above, where the relative energy of the MLCT bands within the series of compounds **1a–3a** and **1b–3b** seem to follow the HOMO–LUMO gap trend. In fact, the hypsochromic shift observed for MLCT bands in the UV–Vis spectra with lengthening of the thiophene ligand is in good agreement with this observation. For all complexes, the Fe(II)/Fe(III) potential is lower in acetonitrile which reflects a relative destabilization of the HOMO when compared to that observed in dichloromethane. The magnitude of this destabilization slightly depends on the phosphine coligand and the extension of the aromatic system. On the other hand, acetonitrile stabilizes the LUMO in all the complexes but the magnitude of this stabilization strongly depends on the phosphine coligand and the extension of the aromatic system. The relative stabilization of the LUMO increases with the chain length of the thiophene ligands. For the compounds with dppe coligand, the relative stabilization corresponds to a difference in the first reduction potential of 20 mV for **1a**, 80 mV for **2a** and 100 mV for **3a**. For the complexes with (+)-diop the relative stabilization of the LUMO is lower: for **1b** no net stabilization was observed whereas for **2b** and **3b** the difference on the first reduction potential was 20 mV and 70 mV, respectively. As a result, the overall effect on the HOMO–LUMO gaps gives lower values in acetonitrile (see Table 4). The difference between the HOMO–LUMO gaps in both solvents and the relative contribution of HOMO (and consequently of LUMO) to the net stabilization observed in acetonitrile is shown in Fig. 5. For the compounds with one thiophene ring (**1a** and **1b**) the lower HOMO–LUMO gaps obtained in acetonitrile are mainly due to the relative destabilization of the HOMO in this solvent (Table 4). For compound **2a**, the net stabilization in acetonitrile has equal contributions of the HOMO destabilization and the LUMO stabilization, whereas for **2b** the main contribution is due to the HOMO destabilization. Finally, for **3a** the net stabilization in acetonitrile is mainly due to the LUMO stabilization whereas for **3b** it has almost equal contribution of HOMO destabilization and LUMO stabilization. This means that as the chain length of the thiophene ligands increases, the stabilization of the LUMO becomes more important for the decrease of the HOMO–LUMO gap in a more polar solvent. Furthermore, this effect is more pronounced with a better donor phosphine (dppe). The lower HOMO–LUMO gaps obtained in acetonitrile compared to dichloromethane agrees with the solvatochromic behaviour of the MLCT bands of the compounds with one and two thiophene units (see above), where a bathochromic shift upon increasing the polarity of the solvent was found. The solvatochromic behaviour of the MLCT band for **3a** and **3b** could not be

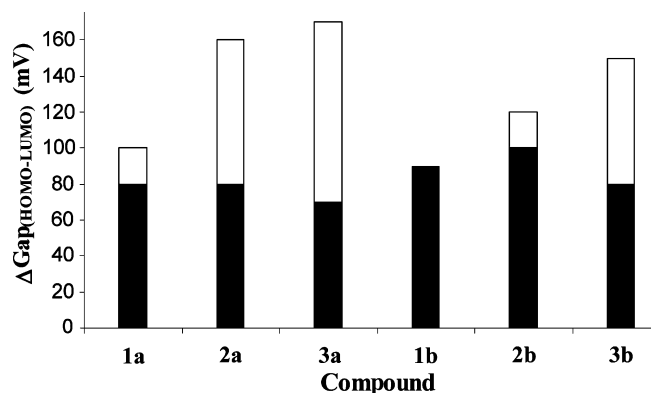


Fig. 5. Difference between HOMO–LUMO gaps in dichloromethane and acetonitrile (taken from Table 4) and the relative contribution of HOMO (black) and LUMO (white) on the net lower gaps observed in acetonitrile ($\Delta\text{Gap}_{(\text{HOMO-LUMO})} = (\text{HOMO-LUMO})_{\text{dichloromethane}} - (\text{HOMO-LUMO})_{\text{acetonitrile}}$).

clearly identified due to an overlapping of this transition with the one attributed to the coordinated thiophene ligand. However, the electrochemical results showed an enhanced stabilization of the LUMO by acetonitrile with the extension of the aromatic thiophene system, which indicates a large dipole moment variation ($\Delta\mu$) upon (photo-) excitation for the compounds with three thiophene rings, and in particular for **3a**.

The second-order NLO properties of the complexes with dppe coligand (**1a–3a**) were studied by HRS measurements at two different fundamental wavelengths of 1.064 and 1.550 μm . The obtained molecular first hyperpolarizabilities β are summarized in Table 5, in which also the most relevant related iron benzonitrile complexes are introduced for comparison.

Because compounds **1a–3a** exhibit an optical transition in the visible range, the β values at 1.064 μm are strongly affected by two-photon resonant enhancement. The well-known two-level model (TLM) of Oudar and Chemla [30], which is very often used in the literature to derive static values, β_0 , is expected to become invalid close to resonance as it ignores any kind of line-broadening mechanisms. This model, in which it is assumed that the lowest energy CT transition yields the dominant contribution to β , diverges whenever the (laser or) second-harmonic wavelength approaches the transition wavelength. This can lead to a strong overestimation of the resonance effect and hence a significant underestimation of the static first hyperpolarizability. Therefore, additional measurements were performed at a longer fundamental wavelength of 1.550 μm , outside of the long wavelength absorption band of each of the compounds, where reasonable results can be expected from the TLM analysis. In this way, the effects of resonant enhancement and increasing conjugation length are disentangled, enabling the formulation of reliable relations between molecular structure and NLO properties. With this in mind, the static values β_0 (see Table 5), calculated using the TLM based on the long wavelength β

Table 5
Experimental first hyperpolarizabilities (β) and chemical structures of the compounds referred in the text

No.	Compound	β_{zzz} at 1.064 μm	β_{zzz} at 1.550 μm	λ_{eg} (nm) ^a	$\beta_{zzz,0}^b$
1a	[FeCp(dppe)(NC{SC ₄ H ₂ }NO ₂)] ⁺	455	255	579	97
2a	[FeCp(dppe)(NC{SC ₄ H ₂ } ₂ NO ₂)] ⁺	710	177	535	82
3a	[FeCp(dppe)(NC{SC ₄ H ₂ } ₃ NO ₂)] ⁺	910	185	460	109
5a	[FeCp(dppe)(NC{C ₆ H ₄ }NO ₂)] ⁺	375 ^c			
6a	[FeCp(dppe)(NC{C ₆ H ₄ } ₂ NO ₂)] ⁺	240 ^c			

All measurements are performed in CHCl₃ solution. The β values are expressed in 10⁻³⁰ esu.

^a λ_{eg} is the position of the longest wavelength absorption band obtained from a fit with multiple Gaussian bands.

^b β_0 based on β_{zzz} at 1.550 μm , using the two-level model with λ_{eg} .

^c Ref. [9].

values, will be used in the upcoming discussion of the experimental results. For the calculation of the β_0 values, the position of the longest wavelength absorption band obtained from a fit with multiple Gaussian bands is used as λ_{eg} . Of course, because of the composite structure of the absorption bands, the choice of λ_{eg} is somewhat arbitrary within the range of the low-energy electronic transitions. This determination influences the exact β_0 values, but the general trends and conclusions discussed below are quite insensitive to the precise value of λ_{eg} .

From the experimental HRS data in Table 5, it appears that the thiophene derivatives studied in this work generally yield higher resonant β values than the related *p*-substituted benzonitrile based complexes (compare **1a** to **5a** and **2a** to **6a**). This is attributed to a higher degree of π -backdonation from the Fe(II) organometallic fragment to the thiophene ligands leading to a more effective extension of conjugation from the metal centre to the electron acceptor NO₂ group, as evidenced from the spectroscopic (IR, NMR) and electrochemical data discussed above. The correlation between the magnitude of β and the π -backdonation process was previously addressed for systematic variation of the metal ion in the related benzonitrile complexes [9]. Table 5 also shows a steady increase in resonant β values at 1.064 μm with increasing number of thiophene units, leading to the large value of 910×10^{-30} esu for **3a**. The less resonant β values at 1.550 μm , however, are not following this trend, and neither do their derived static values which are practically equal for all three thiophenes under study. So, apparently the present complexes are not exhibiting the usual evolution of increasing β with conjugation length, as reported for purely organic push-pull molecules [14,15]. As discussed before, the oligo-thiophene torsion angles are expected to be too small to be a significant factor in the observed trend. Hence, the constancy of the static β values with increasing length of the thiophene chain must be attributed to a competition between the growing conjugation length, which tends to raise β , and a decrease of the CT efficiency having a β lowering effect. Apparently, the use of longer conjugated chains is affecting the coupling between the organometallic donor moiety and the nitro acceptor group, more than for typical organic push-pull systems. The fact that the CT is hampered in case of longer thiophene chains is also seen from

the spectroscopic and electrochemical measurements, which all indicated a decrease of π -backdonation for longer conjugated ligands (see above). These observations demonstrate very clearly that resonantly enhanced values at 1.064 μm can be extremely deceiving, as they seem to indicate that compounds **1a–3a** follow the traditional trend of increasing β with longer conjugated chain. It is observed that β increases much less upon going from 1.550 μm to 1.064 μm for **1a** than for **2a** and **3a**. This behaviour cannot be explained by the difference in resonance conditions (values of λ_{eg} relative to 532 nm: **1a** is closer to resonance than **3a**), within the TLM, not even if homogeneous damping [31] is taken into account. Clearly, near to resonance the dispersion of the β values of compounds **1a–3a** is not well described by this simple model. This discrepancy cannot be accounted for by the uncertainty in λ_{eg} , since the longest wavelength component in the spectrum was chosen, which yields the most conservative estimate of the resonance effect. Indeed, note that if a spectral component at shorter λ_{eg} value was selected, β values at 1.072 μm would be even more resonant for **1a** and less resonant for **2a** and **3a**. Possibly, the discrepancy is caused by a red shift between the β dispersion and the linear absorption maximum, as reported for an organic chromophore [32] and also observed in wavelength dependent HRS for an iron nitrile complex [33]. Because the behaviour of β in the resonance regime is not well understood, measurements outside of this region are required in order to formulate dependable structure–NLO properties relationships.

To analyze the different factors contributing to β we can make use of the above-mentioned TLM [30], according to which β_0 depends on the frequency and oscillator strength of the electronic transition (usually approximated by (the position of) the maximum of the lowest energy absorption band) and the difference in dipole moment between the ground and the CT-excited state $\Delta\mu$. Indeed, a decrease of the first hyperpolarizability with increasing HOMO–LUMO gaps (higher CT-transition frequency), was observed for η^5 -monocyclopentadienylmetal complexes with *p*-benzonitrile ligands [10,34]. A longer conjugated chain favours larger oscillator strength (see Fig. 2) and $\Delta\mu$, if the same amount of charge transfer can still be achieved. Information on $\Delta\mu$ can be obtained from the solvatochromic studies, where a bathochromic shift of the

lower energy CT band was observed for the compounds **1a** and **2a** (see above), indicating an increase of the dipole moment upon excitation ($\Delta\mu > 0$). However, no clear trend in $\Delta\mu$ with increasing chain length can be concluded from the solvatochromism, also because no significant solvatochromic effect was observed for **3a**, due to an overlapping of the MLCT band with an intra-ligand CT band. Anyway, the electrochemical studies presented above seem to indicate that a large $\Delta\mu$ can be expected for this compound. Hence, in terms of the TLM, the increase of β with larger oscillator strength (see Fig. 2) and possibly $\Delta\mu$ for longer thiophene chains, is cancelled by the β lowering effect of the higher CT-transition frequency [and higher HOMO–LUMO gap (see Table 4), the lowest energy transition shifts to higher energies with increasing conjugation length (see Table 1)], and the lower amount of charge transferred. So it seems that both oscillator strength and dipole moment variation upon excitation $\Delta\mu$ play an important role in the second-order nonlinear optical properties of the compounds studied in this work.

The spectroscopic and electrochemical data discussed above also indicate that comparable, or somewhat lower, β values can be expected by replacing the dppe coligand by the chiral (+)-diop phosphine, as was also observed for the related complexes with *p*-substituted benzonitrile ligands [10,34]. Indeed, when comparing to the dppe complexes, the (+)-diop compounds have higher HOMO–LUMO gaps (Table 4). In addition, the electrochemical data in dichloromethane and acetonitrile show that the decreasing HOMO–LUMO gap observed in the more polar solvent is to a larger extent due to the stabilization of the LUMO for the complexes with dppe (Fig. 5), which can lead to higher $\Delta\mu$. In spite of the somewhat lower β values expected for the (+)-diop complexes, the use of this chiral coligand is important in order to obtain a non-centrosymmetrical crystal structure, required for applications in second-order NLO.

3. Conclusion

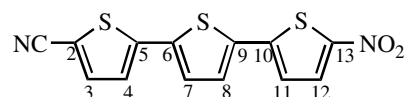
A new class of compounds for second-order NLO materials was developed, combining the organometallic donor fragment FeCp(P₂) (P₂ = dppe, (+)-diop) with conjugated thiophene derived ligands. Spectroscopic and cyclic voltammetry data suggest an improved electronic π -coupling between the η^5 -cyclopentadienyliron fragment and the π -system of the conjugated thiophene ligands, when compared to the previously reported *p*-benzonitrile analogues. Quadratic hyperpolarizabilities of the compounds with dppe have been determined by HRS measurements at two different fundamental wavelengths of 1.064 and 1.550 μm , revealing the two-photon resonance effect and leading to more dependable static values β_0 . These measurements show that the resonant first hyperpolarizabilities at 1.064 μm are indeed higher than for the related benzonitrile compounds, and they can be scaled up by increasing the conjugation length, leading to the high $\beta = 910$

$\times 10^{-30}$ esu for the compound with three thiophene units. The static values, however, are not following the usual evolution of increasing β with conjugation length and are practically independent of the number of thiophene units in the conjugated ligand. Based on the electrochemical and spectroscopic studies it is concluded that this constancy of β upon chain-lengthening is caused by a compensation of the favourable effects of increasing conjugation length by a lowering of the CT efficiency. The present results also demonstrate that resonantly enhanced β values can be extremely deceiving in the evaluation of the molecular NLO-behaviour, as the wavelength-dependence of β within the resonance region is clearly different from the simple two-level models. HRS measurements performed both on- and off-resonance can lead to a better understanding of the behaviour of β in the resonance region and hence an improved modelling of the β dispersion.

4. Experimental

4.1. General procedures

All preparations and manipulations for the synthesis of the complexes described in this work were carried out under nitrogen or argon atmosphere using standard Schlenk techniques. Solvents were purified according to the usual methods [35]. Solid state IR spectra were taken on a Perkin–Elmer 457 spectrophotometer with KBr pellets; only significant bands are cited in the text. ^1H , ^{13}C and ^{31}P NMR spectra were recorded on a Varian Unity 300 spectrometer at probe temperature. The ^1H and ^{13}C resonances are reported in parts per million (ppm) downfield from internal Me₄Si and the ^{31}P NMR spectra are reported in ppm downfield from external standard 85% H₃PO₄. Coupling constants are reported in Hz. Spectral assignments follow the numbering scheme shown below:



Electronic spectra were recorded at room temperature on a Shimadzu UV-1202 spectrometer. Melting points were obtained using a Reichert Thermovar. The molar conductivities of 1 mM solutions of the complexes in nitromethane were recorded with a Schott CGB55 Konduktometer at room temperature. Microanalyses were performed using a Fisons Instruments EA1108 system. Data acquisition, integration and handling were performed using a PC with the software package Eager-200 (Carbo Erba Instruments).

5-Nitro-2-thiophenecarboxaldehyde, 2,2'-bithiophene and 2,2':5',2''-terthiophene were purchased from Aldrich. 2,2'-Bithiophene-5-carboxaldehyde and 2,2':5',2''-terthiophene-5-carboxaldehyde were prepared by Vilsmeier reaction from 2,2'-bithiophene and 2,2':5',2''-terthiophene,

respectively, as described in the literature [36]. 2,2'-Bithiophene-5-carbonitrile and 2,2':5',2''-terthiophene-5-carbonitrile were prepared as described below for **L1** from 2,2'-bithiophene-5-carboxaldehyde and 2,2':5',2''-terthiophene-5-carboxaldehyde, respectively, by formation of the corresponding oximes and dehydration in situ. The nitrating agent, the clay-supported cupric nitrate (*claycop*), was prepared according to previously described [37]. [FeCp(dppe)I] and [FeCp(+)-diop]I were prepared by UV irradiation of a solution of [FeCp(CO)₂] in the presence of the appropriate phosphine in benzene. [FeCp(dppe)NCMe][PF₆] (**4a**) and [FeCp(+)-diop]NCMe][PF₆] (**4b**) were prepared by iodide abstraction of [FeCp(P_P)I] (P_P = dppe or (+)-diop) with TIPF₆ in acetonitrile at room temperature.

4.2. Synthesis of 5-nitrothiophene-2-carbonitrile (**L1**) [30]

5-Nitro-2-thiophenecarboxaldehyde (7.8 g, 0.05 mol) was dissolved in pyridine (20 ml) and hydroxylamine hydrochloride (6.9 g, 0.1 mol) in the same solvent (20 ml) was added. Acetic anhydride (23 ml) was then added and the mixture heated to reflux for 1 h. After cooling, the mixture was poured onto ice and the precipitate formed was filtered, washed with water, dissolved in diethyl ether and dried over sodium sulfate. The solvent was removed under vacuum and the solid was extracted in a Soxhlet apparatus with *n*-pentane to give 6.3 g (82%) of the desired product as yellow needles.

IR (KBr) cm⁻¹: ν(N≡C) 2225; ν(NO₂) 1515 and 1335; δ(NO₂) 730; ¹H NMR (CDCl₃): δ 7.59 (d, 1H, H3, ³J_{HH} = 4.5), 7.91 (d, 1H, H4, ³J_{HH} = 4.2); ¹³C NMR (CDCl₃): δ 111.93 (C2), 115.43 (NC), 127.54 (C4), 136.37 (C3), 155.62 (C5); UV-Vis (CH₂Cl₂): λ_{max}/nm (ε/M⁻¹ cm⁻¹) 301 (10200).

4.3. Synthesis of 5'-nitro-2,2'-bithiophene-5-carbonitrile (**L2**)

2,2'-Bithiophene-5-carbonitrile (5.7 g, 0.03 mol) was added to a suspension of *claycop* (12.6 g) in acetic anhydride (37 ml) below 5 °C with vigorous stirring. Subsequently, the reaction mixture was allowed to achieve the room temperature and stirred for 1 h. The mixture was poured onto ice and the precipitate formed was filtered, washed with dichloromethane and filtered again to separate the clay. The filtrate was washed with a saturated solution of NaHCO₃ and water, dried with Na₂SO₄ and the solvent was removed under vacuum giving a yellow solid as a mixture of 5'-nitro-2,2'-bithiophene-5-carbonitrile (90%) and 4'-nitro-2,2'-bithiophene-5-carbonitrile (10%). The two isomers were separated by fractioned recrystallization from ethanol giving 5.5 g (78%) of the desired compound as a yellow microcrystalline solid.

IR (KBr) cm⁻¹: ν(N≡C) 2220; ν(NO₂) 1520 and 1335; δ(NO₂) 730; ¹H NMR (CDCl₃): δ 7.22 (d, 1H, H7, ³J_{HH} = 4.2), 7.33 (d, 1H, H4, ³J_{HH} = 3.9), 7.61 (d, 1H, H3, ³J_{HH} = 3.9), 7.89 (d, 1H, H8, ³J_{HH} = 4.2); ¹³C NMR

(CDCl₃): δ 110.96 (C2), 113.20 (NC), 124.68 (C7), 126.06 (C4), 129.35 (C8), 138.37 (C3), 141.30 (C5), 141.39 (C6), 151.46 (C9); UV-Vis (CH₂Cl₂): λ_{max}/nm (ε/M⁻¹ cm⁻¹) 377 (22000).

4.4. Synthesis of 5''-nitro-2,2':5',2''-terthiophene-5-carbonitrile (**L3**)

As described above for **L2** from 2,2':5',2''-terthiophene-5-carbonitrile (1.0 g, 3.7 mmol), *claycop* (1.5 g) and acetic anhydride (5 ml). The same workup of the reaction mixture gives 5''-nitro-2,2':5',2''-terthiophene-5-carbonitrile (80%) and 4''-nitro-2,2':5',2''-terthiophene-5-carbonitrile (20%) isomers which were separated by fractioned recrystallization from ethanol. The desired product (0.77 g, 65% yield) was thus obtained as a red microcrystalline solid.

IR (KBr) cm⁻¹: ν(N≡C) 2190; ν(NO₂) 1485 and 1325; δ(NO₂) 750; ¹H NMR (CD₂Cl₂): δ 7.16 (d, 1H, H11, ³J_{HH} = 3.9), 7.23 (d, H, H3, ³J_{HH} = 3.9), 7.29 (d, 1H, H7, ³J_{HH} = 3.9), 7.35 (d, 1H, H8, ³J_{HH} = 3.9), 7.58 (d, 1H, H4, ³J_{HH} = 3.9), 7.87 (d, 1H, H12, ³J_{HH} = 4.5); ¹³C NMR (CD₂Cl₂): δ 109.02 (C2), 114.11 (NC), 123.62 (C8), 124.84 (C7), 127.44 (C4), 127.95 (C11), 130.19 (C12), 136.18 (C9), 137.24 (C6), 138.91 (C3), 143.36 (C5), 144.06 (C10), 150.29 (C13); UV-Vis (CH₂Cl₂): λ_{max}/nm (ε/M⁻¹ cm⁻¹) 426 (37300).

4.5. Synthesis of [FeCp(P_P)(NC{SC₄H₂}_nNO₂)] [PF₆]

All the complexes (P_P = dppe or (+)-diop; *n* = 1, 2 or 3) were prepared as follows. TIPF₆ (0.48 mmol) was added to a solution of [FeCp(P_P)I] (0.40 mmol) and the appropriate nitrile derivative (0.48 mmol) in dichloromethane (20 ml). The suspension was stirred at room temperature for 48–96 h. A change was observed from dark-violet to reddish with simultaneous precipitation of TII. After filtration, the solvent was evaporated under vacuum and the solid residue washed several times with diethyl ether/dichloromethane mixture to remove the excess of the ligand. The obtained solid was recrystallized from dichloromethane/*n*-pentane or *n*-hexane affording the desired complexes almost as dark red microcrystalline products.

¹H and ¹³C NMR data relative to the dppe and (+)-diop coordinated phosphines are very similar in all compounds, and are described below.

Compounds 1a and 2a. For dppe: ¹H NMR (CDCl₃): δ 2.40–2.70 (m, 4H, CH₂), 7.27–7.36 (m, 4H, C₆H₅), 7.48–7.64 (m, 12H, C₆H₅), 7.78–7.86 (m, 4H, C₆H₅); ¹³C NMR (CDCl₃): δ 28.07 (t, CH₂, ¹J_{CP} = 21.4), 129.31 and 129.66 (t, C_{meta}, ³J_{CP} = 4.9), 130.80 and 131.37 (s, C_{para}), 131.08 and 132.67 (t, C_{ortho}, ²J_{CP} = 4.8), 136.24 (t, C_{ipso}, ¹J_{CP} = 20.7).

Compound 3a. For dppe: ¹H NMR (CD₂Cl₂): δ 2.40–2.70 (m, 4H, CH₂), 7.32–7.38 (m, 4H, C₆H₅), 7.48–7.54 (m, 6H, C₆H₅), 7.58–7.66 (m, 6H, C₆H₅), 7.80–7.88 (m, 4H, C₆H₅); ¹³C NMR (CD₂Cl₂): δ 28.10 (t, CH₂,

$^1J_{\text{CP}} = 21.4$), 129.64 and 129.82 (t, C_{meta} , $^3J_{\text{CP}} = 4.9$), 131.66 and 131.66 (s, C_{para}), 131.60 and 133.02 (t, C_{orto} , $^2J_{\text{CP}} = 4.9$), 136.50 (t, C_{ipso} , $^1J_{\text{CP}} = 22.4$).

Compounds 1b and 2b. For (+)-diop: ^1H NMR (CDCl_3): δ 1.09 (s, 3H, CH_3), 1.27 (s, 3H, CH_3), 2.24–2.36 (m, 2H, CH_2), 3.03–3.18 (m, 2H, CH_2), 3.20–3.28 (m, 1H, CH), 3.42–3.52 (m, 1H, CH), 7.20–7.27 (m, 4H, C_6H_5), 7.44–7.52 (m, 6H, C_6H_5), 7.63 (t, 4H, C_6H_5 , $^3J_{\text{HH}} = 8.5$), 7.74 (t, 4H, C_6H_5 , $^3J_{\text{HH}} = 7.5$), 8.02 (t, 2H, C_6H_5 , $^3J_{\text{HH}} = 8.6$); ^{13}C NMR (CDCl_3): δ 26.68 (s, CH_3), 26.85 (s, CH_3), 28.42 (d, CH_2 , $^1J_{\text{CP}} = 18.7$), 30.92 (d, CH_2 , $^1J_{\text{CP}} = 27.0$); 75.25 (d, CH, $^2J_{\text{CP}} = 11.0$), 78.06 (d, CH, $^2J_{\text{CP}} = 7.2$), 109.14 (s, $\text{C}(\text{CH}_3)_2$), 128.86–134.21 (m, C_6H_5), 138.22 (d, C_{ipso} , $^1J_{\text{CP}} = 42.9$), 141.32 (d, C_{ipso} , $^1J_{\text{CP}} = 47.0$).

Compound 3b. For (+)-diop: ^1H NMR (CD_2Cl_2): δ 1.00 (s, 3H, CH_3), 1.20 (s, 3H, CH_3), 2.22–2.37 (m, 2H, CH_2), 3.01–3.17 (m, 2H, CH_2), 3.21–3.32 (m, 1H, CH), 3.37–3.53 (m, 1H, CH), 7.32–7.80 (m, 18H, C_6H_5), 7.96–8.07 (m, 2H, C_6H_5); ^{13}C NMR (CD_2Cl_2): δ 26.80 (s, CH_3), 26.93 (s, CH_3), 28.70 (d, CH_2 , $^1J_{\text{CP}} = 18.0$), 31.32 (d, CH_2 , $^1J_{\text{CP}} = 20.7$), 75.42 (d, CH, $^2J_{\text{CP}} = 11.0$), 78.39 (d, CH, $^2J_{\text{CP}} = 7.2$), 109.46 (s, $\text{C}(\text{CH}_3)_2$), 129.40–134.65 (m, C_6H_5), 138.80 (d, C_{ipso} , $^1J_{\text{CP}} = 42.2$), 141.27 (d, C_{ipso} , $^1J_{\text{CP}} = 42.0$).

4.5.1. [*FeCp(dppe)(NC{SC₄H₂}NO₂)][PF₆] (1a)*

Dark red; recrystallized from $\text{CH}_2\text{Cl}_2/n$ -pentane; 56% yield; m.p. 220 °C (dec.); molar conductivity ($\Omega^{-1}\text{cm}^2\text{mol}^{-1}$) 75.3; IR (KBr) cm^{-1} : $\nu(\text{N}\equiv\text{C})$ 2190; ^1H NMR (CDCl_3): δ 4.55 (s, 5H, $\eta^5\text{-C}_5\text{H}_5$), 6.98 (d, 1H, H3, $^3J_{\text{HH}} = 4.2$), 7.61 (d, 1H, H4, $^3J_{\text{HH}} = 4.2$); ^{13}C NMR (CDCl_3): δ 81.03 ($\eta^5\text{-C}_5\text{H}_5$), 114.00 (C2), 125.14 (NC), 128.22 (C4), 138.22 (C3), 153.54 (C5); ^{31}P NMR (CDCl_3): δ 97.22. Anal. Calc. for $\text{C}_{36}\text{H}_{31}\text{F}_6\text{N}_2\text{O}_2\text{P}_3\text{SFe}$: C, 52.83; H, 3.82, N, 3.42; S, 3.92. Found: C, 52.55; H, 3.80, N, 3.30; S, 4.01%.

4.5.2. [*FeCp(dppe)(NC{SC₄H₂}₂NO₂)][PF₆] (2a)*

Dark red; recrystallized from $\text{CH}_2\text{Cl}_2/n$ -hexane; 48% yield; m.p. 230 °C (dec.); molar conductivity ($\Omega^{-1}\text{cm}^2\text{mol}^{-1}$) 74.9; IR (KBr) cm^{-1} : $\nu(\text{N}\equiv\text{C})$ 2200; ^1H NMR (CDCl_3): δ 4.50 (s, 5H, $\eta^5\text{-C}_5\text{H}_5$), 6.76 (d, 1H, H3, $^3J_{\text{HH}} = 4.2$), 7.07 (d, 1H, H4, $^3J_{\text{HH}} = 4.2$), 7.11 (d, 1H, H7, $^3J_{\text{HH}} = 4.2$), 7.83 (d, 1H, H8, $^3J_{\text{HH}} = 4.5$); ^{13}C NMR (CDCl_3): δ 80.24 ($\eta^5\text{-C}_5\text{H}_5$), 110.14 (C2), 125.01 (C7), 126.42 (C4), 127.00 (NC), 128.04 (C8), 139.91 (C3), 140.51 (C5), 140.90 (C6), 151.07 (C9); ^{31}P NMR (CDCl_3): δ 97.49. Anal. Calc. for $\text{C}_{40}\text{H}_{33}\text{F}_6\text{N}_2\text{O}_2\text{P}_3\text{S}_2\text{Fe}$: C, 53.35; H, 3.69, N, 3.11; S, 7.12. Found: C, 52.98; H, 3.74, N, 3.02; S, 6.98%.

4.5.3. [*FeCp(dppe)(NC{SC₄H₂}₃NO₂)][PF₆] (3a)*

Brownish-red; recrystallized from $\text{CH}_2\text{Cl}_2/n$ -hexane; 40% yield; m.p. 179–180 °C; molar conductivity ($\Omega^{-1}\text{cm}^2\text{mol}^{-1}$) 71.2; IR (KBr) cm^{-1} : $\nu(\text{N}\equiv\text{C})$ 2210; ^1H NMR (CD_2Cl_2): δ 4.49 (s, 5H, $\eta^5\text{-C}_5\text{H}_5$), 6.50 (d, 1H,

H3, $^3J_{\text{HH}} = 4.2$), 6.96 (d, 1H, H4, $^3J_{\text{HH}} = 3.9$), 7.15 (d, 1H, H11, $^3J_{\text{HH}} = 4.5$), 7.17 (d, 1H, H7, $^3J_{\text{HH}} = 4.5$), 7.32 (d, 1H, H8, $^3J_{\text{HH}} = 4.2$), 7.85 (d, 1H, H12, $^3J_{\text{HH}} = 4.5$); ^{13}C NMR (CD_2Cl_2): δ 80.40 ($\eta^5\text{-C}_5\text{H}_5$), 107.75 (C2), 123.82 (C8), 124.58 (C7), 127.76 (C11), 128.06 (C4), 129.32 (NC), 130.26 (C12), 136.54 (C9), 136.70 (C6), 139.59 (C3), 143.71 (C10), 143.88 (C5), 150.29 (C13); ^{31}P NMR (CD_2Cl_2): δ 97.63. Anal. Calc. for $\text{C}_{44}\text{H}_{35}\text{F}_6\text{N}_2\text{O}_2\text{P}_3\text{S}_3\text{Fe}$: C, 53.78; H, 3.59, N, 2.85; S, 9.79. Found: C, 53.47; H, 3.39, N, 2.73; S, 9.54%.

4.5.4. [*FeCp((+)-diop)(NC{SC₄H₂}NO₂)][PF₆] (1b)*

Dark red; recrystallized from $\text{CH}_2\text{Cl}_2/n$ -pentane; 37% yield; m.p. 185 °C (dec.); molar conductivity ($\Omega^{-1}\text{cm}^2\text{mol}^{-1}$) 77.4; IR (KBr) cm^{-1} : $\nu(\text{N}\equiv\text{C})$ 2180; ^1H NMR (CDCl_3): δ 4.23 (s, 5H, $\eta^5\text{-C}_5\text{H}_5$), 7.80 (d, 1H, H3, $^3J_{\text{HH}} = 4.2$), 7.85 (d, 1H, H4, $^3J_{\text{HH}} = 4.2$); ^{13}C NMR (CDCl_3): δ 82.53 ($\eta^5\text{-C}_5\text{H}_5$), 113.99 (C2), 127.76 (NC), 128.71 (C4), 139.22 (C3), 154.07 (C5); ^{31}P NMR (CDCl_3): δ 53.3 (2d, $J_{\text{PA}P_{\text{B}}} = 47.4$). Anal. Calc. for $\text{C}_{41}\text{H}_{39}\text{F}_6\text{N}_2\text{O}_4\text{P}_3\text{SFe}$: C, 53.61; H, 4.28, N, 3.05; S, 3.49. Found: C, 53.43; H, 4.35, N, 2.97; S, 3.37%.

4.5.5. [*FeCp((+)-diop)(NC{SC₄H₂}₂NO₂)][PF₆] (2b)*

Dark red; recrystallized from $\text{CH}_2\text{Cl}_2/n$ -pentane; 32% yield; m.p. 140–142 °C; molar conductivity ($\Omega^{-1}\text{cm}^2\text{mol}^{-1}$) 72.6; IR (KBr) cm^{-1} : $\nu(\text{N}\equiv\text{C})$ 2190; ^1H NMR (CDCl_3): δ 4.16 (s, 5H, $\eta^5\text{-C}_5\text{H}_5$), 7.20 (d, 1H, H7, $^3J_{\text{HH}} = 4.2$), 7.31 (d, 1H, H3, $^3J_{\text{HH}} = 4.5$), 7.54 (d, 1H, H4, $^3J_{\text{HH}} = 4.2$), 7.85 (d, 1H, H8, $^3J_{\text{HH}} = 4.2$); ^{13}C NMR (CDCl_3): δ 81.76 ($\eta^5\text{-C}_5\text{H}_5$), 109.35 (C2), 125.29 (C7), 126.99 (C4), 128.29 (C8), 129.48 (NC), 140.51 (C3), 141.12 (C5), 141.17 (C6), 151.30 (C9); ^{31}P NMR (CDCl_3): δ 53.7 (2d, $J_{\text{PA}P_{\text{B}}} = 47.4$). Anal. Calc. for $\text{C}_{45}\text{H}_{41}\text{F}_6\text{N}_2\text{O}_4\text{P}_3\text{S}_2\text{Fe}$: C, 54.01; H, 4.13, N, 2.80; S, 6.41. Found: C, 53.93; H, 4.01, N, 2.88; S, 6.25%.

4.5.6. [*FeCp((+)-diop)(NC{SC₄H₂}₃NO₂)][PF₆] (3b)*

Brownish-red; recrystallized from $\text{CH}_2\text{Cl}_2/n$ -pentane; 28% yield; m.p. 134–136 °C; molar conductivity ($\Omega^{-1}\text{cm}^2\text{mol}^{-1}$) 69.8; IR (KBr) cm^{-1} : $\nu(\text{N}\equiv\text{C})$ 2190; ^1H NMR (CD_2Cl_2): δ 4.08 (s, 5H, $\eta^5\text{-C}_5\text{H}_5$), 7.16 (d, 1H, H11, $^3J_{\text{HH}} = 4.5$), 7.18 (d, 1H, H3, $^3J_{\text{HH}} = 4.2$), 7.25 (d, 1H, H7, $^3J_{\text{HH}} = 4.2$), 7.26 (d, 1H, H4, $^3J_{\text{HH}} = 3.9$), 7.33 (d, 1H, H8, $^3J_{\text{HH}} = 3.9$), 7.86 (d, 1H, H12, $^3J_{\text{HH}} = 4.2$); ^{13}C NMR (CD_2Cl_2): δ 81.78 ($\eta^5\text{-C}_5\text{H}_5$), 107.48 (C2), 123.93 (C8), 125.17 (C7), 128.09 (C11), 128.11 (C4), 130.40 (C12), 132.02 (NC), 136.45 (C9), 136.94 (C6), 140.07 (C3), 143.71 (C10), 144.66 (C5), 150.51 (C13); ^{31}P NMR (CD_2Cl_2): δ 53.4 (2d, $J_{\text{PA}P_{\text{B}}} = 47.4$). Anal. Calc. for $\text{C}_{49}\text{H}_{43}\text{F}_6\text{N}_2\text{O}_4\text{P}_3\text{S}_3\text{Fe}$: C, 54.35; H, 4.00, N, 2.59; S, 8.88. Found: C, 54.19; H, 3.91, N, 2.48; S, 8.74%.

4.6. Electrochemical experiments

The electrochemistry instrumentation consisted of a EG&A Princeton Applied Research Model 273A

Potentiometer and experiments were monitored with a PC computer loaded with Model 270 Electrochemical Analysis Software 3.00 of EG&A from Princeton Applied Research. Potentials were referred to a calomel electrode containing a saturated solution of potassium chloride. The working electrode was a 2-mm piece of platinum wire for voltammetry. The secondary electrode was a platinum wire coil. Cyclic voltammetry experiments were performed at room temperature and $-20\text{ }^{\circ}\text{C}$ in a PAR polarographic cell. Solutions studied were 1 mM in solute and 0.1 M in tetrabutylammonium hexafluorophosphate as supporting electrolyte. The electrochemical system was checked with a 1 mM solution of ferrocene in acetonitrile and dichloromethane for which the ferrocinium/ferrocene electrochemical parameters ($E_{p/2} = 0.38\text{ V}$ in acetonitrile and $E_{p/2} = 0.41\text{ V}$ in dichloromethane; $\Delta E = 60\text{--}70\text{ mV}$; $I_a/I_c = 1$) were in good agreement with the literature [38,39].

The electrolyte was purchased from Aldrich Chemical Co., recrystallized from ethanol, washed with diethyl ether, and dried under vacuum at $110\text{ }^{\circ}\text{C}$ for 24 h. Reagent grade acetonitrile and dichloromethane were dried over P_2O_5 and CaH_2 , respectively, and distilled under argon atmosphere before use. An argon atmosphere was also maintained over the solution during the experiments.

4.7. β Measurements

HRS measurements at $1.064\text{ }\mu\text{m}$ were performed using 70 ps pulses from a 2 kHz repetition rate Nd:YAG regenerative amplifier seeded by a mode-locked Nd:YAG laser (as described in Ref. [5]). The scattered second-harmonic light is analyzed with a monochromator, in addition to electronic gating within a 4 ns time window in order to discriminate efficiently between hyper-Rayleigh scattering and (two-photon) luminescence. For the measurements at $1.550\text{ }\mu\text{m}$ a recently developed HRS-setup [33] is used, based on an optical parametrical amplifier (OPA) pumped by a Ti:Sapphire regenerative amplifier, and with single-photon sensitive, parallel detection of a small spectral range around the second-harmonic wavelength. With this setup, measurements were also performed at $1.072\text{ }\mu\text{m}$, reproducing the $1.064\text{ }\mu\text{m}$ β values to within the experimental error of 5%. For the compounds studied here some decomposition in the focused laser beam took place, which was observed in the measurements at $1.064\text{ }\mu\text{m}$ by a slight decrease in HRS intensity (typically in the order of 10%) within a few seconds after the liquid cell was moved to another position relative to the laser beam as well as through a slight deviation from the quadratic power dependence of the HRS signal. This problem was solved by having a magnetic stirrer rotating in the liquid cell during the HRS measurements in order to continuously refresh the solution in the small volume of the laser focus. All measurements are calibrated relative to pure chloroform [40], for which the literature value of 0.49×10^{-30} esu is adopted (EFISHG, from Ref. [41], using the usual assumptions [5]). Because of the very low β dispersion of the pure solvent, it

is a good approximation, within experimental accuracy, to adopt the same value for the two different wavelengths.

Acknowledgements

Financial support from Fundação para a Ciência e Tecnologia (FCT), project POCTI/QUI/48443/2002 and from the Fund for Scientific Research of Flanders (Belgium) (FWO–Vlaanderen) in the group Projects G.0041.01 and G.0129.07 is gratefully acknowledged. W.W. is a Postdoctoral Fellow of the FWO.

References

- [1] H.S. Nalwa, Appl. Organomet. Chem. 5 (1991) 349.
- [2] N.J. Long, Angew. Chem., Int. Ed. Engl. 34 (1995) 21.
- [3] S.R. Marder, in: D.W. Bruce, D. O'Hare (Eds.), Inorganic Materials, second ed., Wiley, Chichester, 1996, p. 121.
- [4] I.R. Whittall, A.M. McDonagh, M.G. Humphrey, M. Samoc, Adv. Organomet. Chem. 42 (1998) 291.
- [5] E. Goovaerts, W.E. Wenseleers, M.H. Garcia, G.H. Cross, in: H.S. Nalwa (Ed.), Handbook of Advanced Electronic and Photonic Materials, vol. 9, Academic Press, San Diego, 2001, p. 127 (Chapter 3).
- [6] S. Di Bella, Chem. Soc. Rev. 30 (2001) 355.
- [7] J.C. Calabrese, L.T. Cheng, J.C. Green, S.R. Marder, W. Tam, J. Am. Chem. Soc. 113 (1991) 7227–7232.
- [8] A. Krishnan, S.K. Pal, P. Nandakumar, A.G. Samuelson, P.K. Das, Chem. Phys. 265 (2001) 313–322.
- [9] W. Wenseleers, A.W. Gerbrandij, E. Goovaerts, M.H. Garcia, M.P. Robalo, P.J. Mendes, J.C. Rodrigues, A.R. Dias, J. Mater. Chem. 8 (1998) 925.
- [10] M.H. Garcia, M.P. Robalo, A.R. Dias, M.F.M. Piedade, A. Galvão, M.T. Duarte, W. Wenseleers, E. Goovaerts, J. Organomet. Chem. 619 (2001) 252.
- [11] M.H. Garcia, M.P. Robalo, A.R. Dias, M.T. Duarte, W. Wenseleers, G. Aerts, E. Goovaerts, M.P. Cifuentes, S. Hurst, M.G. Humphrey, M. Samoc, B. Luther-Davies, Organometallics 21 (2002) 2107.
- [12] C.E. Powell, M.G. Humphrey, Coord. Chem. Rev. 248 (2004) 725.
- [13] M.P. Cifuentes, M.G. Humphrey, J. Organomet. Chem. 689 (2004) 3968.
- [14] J.L. Oudar, H. Leperson, Opt. Commun. 15 (1975) 258–262.
- [15] A. Dulicic, C. Flytzanis, C.L. Tang, D. Pepin, M. Fetizon, Y. Hoppilliard, J. Chem. Phys. 74 (1981) 1559–1563.
- [16] A.M. McDonagh, I.R. Whittall, M.G. Humphrey, B.W. Skelton, A.H. White, J. Organomet. Chem. 519 (1996) 229.
- [17] M. Ciofalo, G. La Manna, Chem. Phys. Lett. 263 (1996) 73.
- [18] T.L. Porter, D. Minore, D. Zhang, J. Phys. Chem. 99 (1995) 13213.
- [19] R.D.A. Hudson, A.R. Manning, D.F. Nolan, I. Asselberghs, R. Van Boxel, A. Persoons, J.F. Gallagher, J. Organomet. Chem. 619 (2001) 141.
- [20] R.D.A. Hudson, I. Asselberghs, K. Clays, L.P. Cuffe, J.F. Gallagher, A.R. Manning, A. Persoons, K. Wostyn, J. Organomet. Chem. 637–639 (2001) 435.
- [21] M.H. Garcia, S. Royer, M.P. Robalo, A.R. Dias, J.-P. Tranchier, R. Chavignon, D. Prim, A. Auffrant, F. Rose-Munch, E. Rose, J. Vaissermann, A. Persoons, I. Asselberghs, Eur. J. Inorg. Chem. (2003) 3895.
- [22] B. Insuasty, C. Atienza, C. Seoane, N. Martín, J. Garin, J. Orduna, R. Alcalá, B. Villacampa, J. Org. Chem. 69 (2004) 6986.
- [23] J.-L. Fillaut, J. Perruchon, P. Blanchard, J. Roncali, S. Golhen, M. Allain, A. Migalska-Zalas, I.V. Kityk, B. Sahraoui, Organometallics 24 (2005) 687.
- [24] Y. Liao, B.E. Eichinger, K.A. Firestone, M. Haller, J. Luo, W. Kaminsky, J.B. Benedict, P.J. Reid, A.K.-Y. Jen, L.R. Dalton, B.H. Robinson, J. Am. Chem. Soc. 127 (2005) 2758.

- [25] A.-L. Roy, M. Chavarot, É. Rose, F. Rose-Munch, A.-J. Attias, D. Kréher, J.-L. Fave, C. Kamierszky, C.R. Chimie 8 (2005) 1256.
- [26] P.M. Theus, W. Weuffen, H. Tiedt, Arch. Pharm. 301 (1968) 139.
- [27] W.J. Geary, Coord. Chem. Rev. 7 (1977) 81.
- [28] A.R. Dias, M.H. Garcia, M.P. Robalo, M.L.H. Green, K.K. Lai, A.J. Pulham, S.M. Klueber, G. Balavoine, J. Organomet. Chem 453 (1993) 241.
- [29] P. Hapiot, F. Demanze, A. Yassar, F. Garnier, J. Phys. Chem. 100 (1996) 8397.
- [30] J.L. Oudar, D.S. Chemla, J. Chem. Phys. 66 (1977) 2664.
- [31] G. Berkovic, G. Meshulam, Z. Kotler, J. Chem. Phys. 112 (2000) 3997.
- [32] C.H. Wang, Y.C. Lin, O.Y. Tai, A.K.-Y. Jen, J. Chem. Phys. 119 (2003) 6237–6244.
- [33] M.P. Robalo, A.P.S. Teixeira, M.H. Garcia, M.F.M. da Piedade, M.T. Duarte, A.R. Dias, J. Campo, W. Wenseleers, E. Goovaerts, Eur. J. Inorg. Chem. 11 (2006) 2175–2185.
- [34] P.J. Mendes, J.P. Prates Ramalho, A.J.E. Candeias, M.P. Robalo, M.H. Garcia, J. Mol. Struct. (Theochem) 729 (2005) 109.
- [35] D.D. Perrin, W.L.F. Amarego, D.R. Perrin, Purification of Laboratory Chemicals, second ed., Pergamon Press, New York, 1980.
- [36] Y. Wei, B. Wang, W. Wang, J. Tian, Tetrahedron Lett. 36 (1995) 665.
- [37] P. Laszlo, A. Cornélis, Aldrichim. Acta 21 (1988) 97.
- [38] I.V. Nelson, R.T. Iwamoto, Anal. Chem. 35 (1961) 867.
- [39] R.R. Gagné, C.A. Koval, G.C. Lisensky, Inorg. Chem. 19 (1980) 2855.
- [40] K. Clays, A. Persoons, Phys. Rev. Lett. 66 (1991) 2980.
- [41] F. Kajzar, I. Ledoux, J. Zyss, Phys. Rev. A 36 (1987) 2210.